THE SYNTHESIS OF MODULAR BLOCK COPOLYMERS

A Thesis
Presented to
The Academic Faculty

by

Mary Nell Higley

In Partial Fulfillment
of the Requirements for the Degree
Master's Degree in Chemistry in the
School of Chemistry and Biochemistry

Georgia Institute of Technology
May 2007

THE SYNTHESIS OF MODULAR BLOCK COPOLYMERS

Approved by:

Dr. Marcus Weck, Advisor
School of Chemistry and Biochemistry
Georgia Institute of Technology

Dr. David Collard
School of Chemistry and Biochemistry
Georgia Institute of Technology

Dr. Christopher W. Jones
School of Chemical and Biomedical Engineering
Georgia Institute of Technology

Date Approved: 5 April 2007

TABLE OF CONTENTS

LIST OF TABLES

LIST OF FIGURES

LIST OF SYMBOLS AND ABBREVIATIONS

CT	Chain-Terminator
CTA	Chain-Transfer Agent
ROMP	Ring-Opening Metathesis Polymerization

SUMMARY

A novel methodology has been developed for the formation of block copolymers that combines ring-opening metathesis polymerization (ROMP) with functional chain-transfer agents (CTAs), functional chain-terminators (CTs) and self-assembly. Telechelic homopolymers of cyclooctene derivatives that are end-functionalized with hydrogen-bonding or metal-coordination sites are formed via the combination of ROMP with a corresponding functional CTA. These telechelic homopolymers are fashioned with a high control over molecular weight and without the need for post-polymerization procedures. The homopolymers undergo fast and efficient self-assembly with their complement homopolymer or small molecule analogues to form block copolymer architectures. The block copolymers have similar association constants to small molecule analogues described in the literature, regardless of size or the nature of the complementary unit or the polymer side-chain. The ROMP of side-chain functionalized norbornene polymers is coupled with functional CTs to produce block copolymer with main- and side-chain self-assembly sites. Combinations of these norbornene polymers with their complement polymer *via* self-assembly produce non-covalent AB type block copolymers fast and efficiently. ABA type block copolymers are realized by combining the difunctional homopolymer formed via the CTA pathway with the CT synthesized mono-functional polymer. These polymers show similar association constants regardless of the sequence of polymer formation.

INTRODUCTION

As polymer technologies such as electronic, optical, and biological materials continue to evolve with ever increasing degrees of structural complexity, the preparation of such materials has become more time consuming and difficult. A central feature, crucial to the implementation of these materials in functional devices, is the facile preparation of complex polymer architectures such as block copolymers that contain well-defined monomer compositions, elaborate architectures, and diverse functionalities.[1] Generally, living polymerization techniques have been employed for the formation of block copolymers. Much of today's research, focused on the synthesis of block copolymers, relies upon living ionic, [2] transition-metal catalyzed[3] and controlled free radical[4] polymerization methods. Although successful, these strategies suffer from a variety of shortcomings including functional group incompatibilities with polymerization conditions as well as low degrees of flexibility in optimizing target structures. One potential solution to overcome these difficulties is implementation of end-group functionalized polymers capable of self-assembling to form complex architectures, including block copolymers (Figure 1).

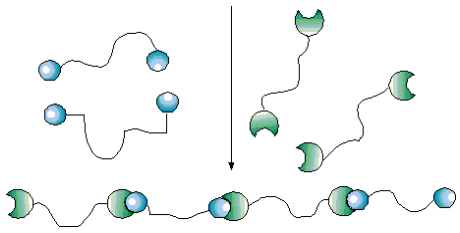

Figure 1. Cartoon depicting the formation of a block copolymer via self-assembly of functional end-groups.

To that end, much recent research efforts have successfully employed metal coordination and hydrogen bonding based recognition motifs for the preparation of self-assembled block copolymers.[5-12] For example, Craig and co-workers successfully incorporated DNA sequences at polymer termini for the preparation of DNA duplex-based self-assembled polymers.[13, 14] The monomers in this system, made from two covalently linked oligonucleotide sequences, resulted in formation of linear polymers that are well suited for studying reversible main-chain self-assembly.[13, 14] In an alternative account, Meijer and co-workers have employed terminal ureidotriazine units (Figure 2) to prepare supramolecular block copolymers with rigid-rod-like and coil-like segments, allowing for facile access to interesting polymer morphologies.[6]

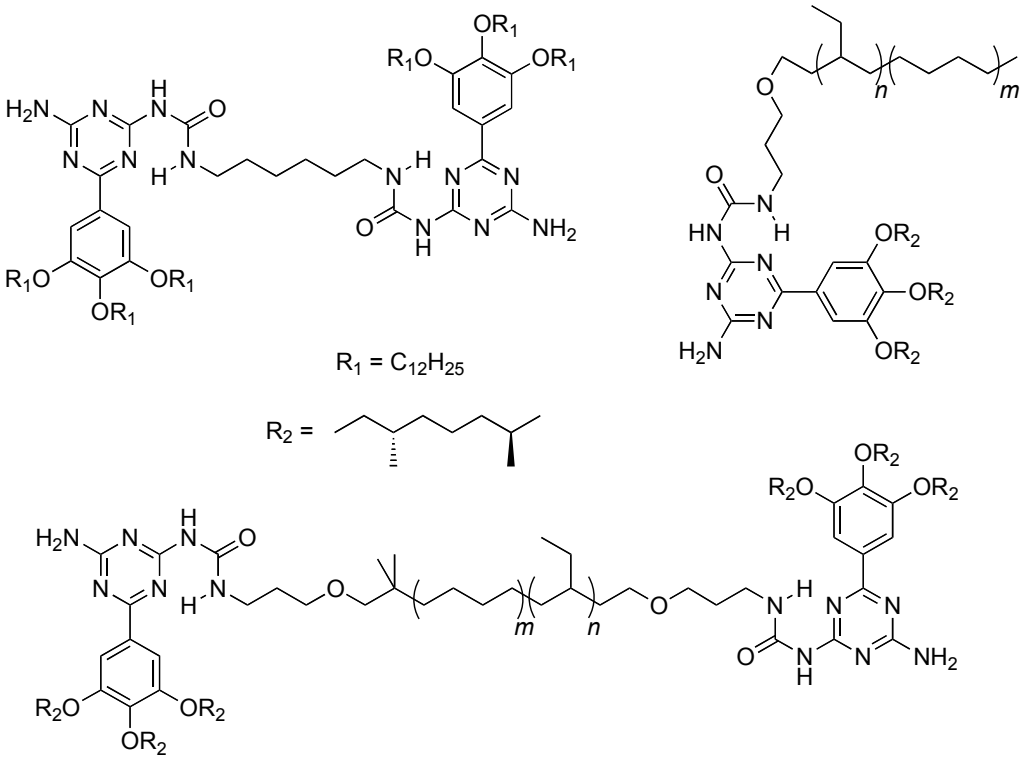

Figure 2. Building blocks for a variety of morphologies employed by Meijer *et al.*

Binder and co-workers affixed of hydrogen-bonding motifs with varying association constants (K_a) to polymer end-groups creating telechelic poly(isobutylene) (PIB) and poly(etherketone) (PEK), and allowing for the formation of supramolecular pseudo-block copolymers (Figure 3).[9]

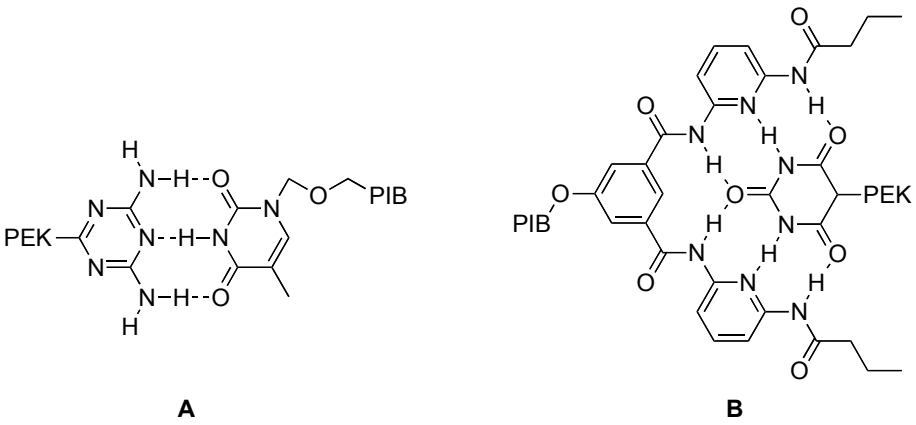

Figure 3. Hydrogen-bonding pairs employed by Binder *et al*, pair **B** is significantly stronger in chloroform than pair **A**.

Other examples include the use of metal coordination for the synthesis of self-assembled block copolymers. For example, Schubert and co-workers have shown that terpyridine units can be incorporated, in a post-polymerization reaction, onto one chain-terminus of commercially available poly(ethyleneoxide), poly(styrene) and poly(ethylene-co-butylene).[15] Using ruthenium, the polymers can be combined to create AB type block copolymers (Figure 4).

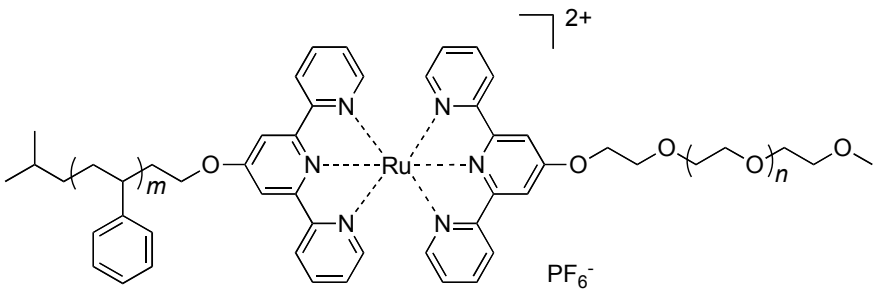

Figure 4. A block copolymer of polystyrene and poly(ethyleneoxide) formed via the metal coordination of end-group terpyridine.

Gerhardt and coworkers assembled fluorescent pyridyl cruciforms with palladium complexes creating supramolecular polymers with optical properties (Figure 5).[10] By altering the ratio of cruciform to palladium complex the degree of polymerization of the supramolecular structures could be modified.[10]

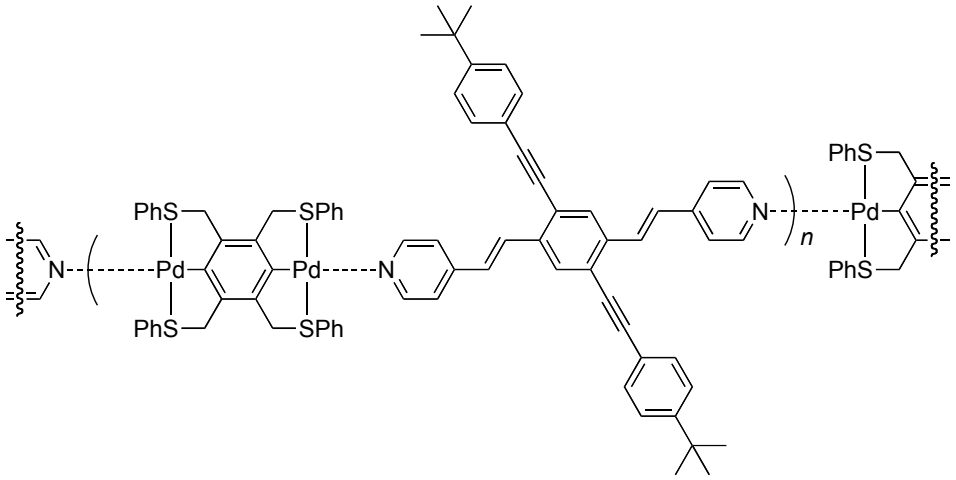

Figure 5. Supramolecular polymer made *via* metal-coordination with the ability to vary the degree of polymerization.

Fraser *et al.* have demonstrated that bipyridine-end-functionalized polymers successfully chelate metal salts to form complex copolymer architectures.[16] Well-

defined bipyridine-functionalized poly(styrene) polymers were prepared via controlled atom-transfer radical polymerization. This system allowed for subsequent metal coordination using ruthenium salts to produce a variety of metal containing block and star copolymers.[15, 16] While these approaches demonstrate the elegant concept of employing metal-coordination to prepare self-assembled polymers, most recognition motifs were incorporated using a post-polymerization step, often without quantitative yield, which limits the versatility and simplicity of this approach. Aside from poor yields, post polymerization based strategies also suffer from functional group incompatibility during the end-group functionalization due to competitive reactions. Furthermore, ruthenium-terpyridine based metal-coordination often requires refluxing ethanol for prolonged reaction times (up to 6 h), greatly limiting this approach to systems capable of tolerating such harsh reaction conditions.

To overcome these shortcomings, a novel strategy has to be devised that allows for 1) rapid and facile end-group functionalization, 2) incorporation of any functional group onto the side-chain of the polymer thereby broadening the scope for preparing complex functional polymeric materials and 3) incorporation of any terminal recognition motif desired. This master thesis introduces such a strategy by combining self-assembly with olefin metathesis. The strategy described herein allows for rapid end-functionalization of homo-polymers possessing recognition motifs that can subsequently self-assemble to create a variety of complex block copolymer structures quickly and efficiently and in a modular fashion (Figure 6).

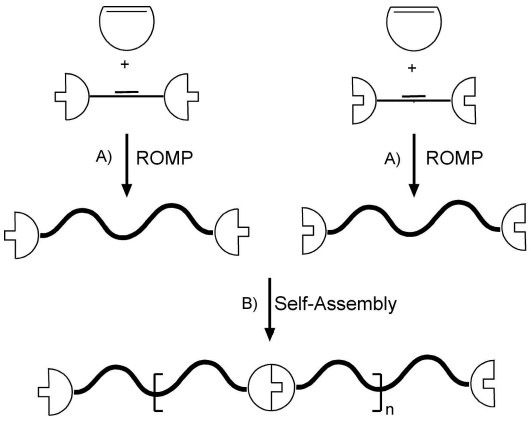

Figure 6. Cartoon depicting A) CTA Polymerization allowing for recognition motif end-functionalization and B) Self-Assembly of the resulting homopolymers.

Complex copolymers are created by combining chain-transfer agents (CTAs), ring-opening metathesis polymerization (ROMP) and self-assembly. Ruthenium catalyzed ROMP is a fully functional group tolerant polymerization technique that allows for the facile introduction of virtually any functional group onto the side-chain.[17] Furthermore, the inclusion of a functionalized chain-transfer agent (CTA) during the course of ROMP allows for complete polymer end-group functionalization and requires no post-polymerization functionalization techniques. By employing CTA's containing different functional end-groups, telechelic polymers possessing any desired recognition motif can be synthesized. Additionally, this methodology allows for control of the molecular weight of the polymer and the polydispersity index (PDI) thereby allowing for unprecedented control over end-group functionalization, polymer properties, and ultimately block copolymer properties.[18-21] Following the CTA assisted preparation of homopolymers possessing complementary recognition units at the chain terminus, rapid

self-assembly via exploitation of non-covalent interactions allows for rapid preparation of a variety of complex telechelic block copolymers.

In chapter 2, the proof of concept is realized and self-assembly of telechelic polymers into linear supramolcular structures is described. Chapter 3 describes the synthesis of other architectures, namely AB and ABA type block-copolymers. To add another degree of complexity to these systems, side-chains with self-assembly recognition sites will be incorporated onto some of the monomers.

Using side-chains to introduce complexity into supramolecular systems has been well studied in recent years[22-27]. Thibault and coworkers used polystyrene as a backbone with hydrogen-bonding motif diamidopyridine as a side-chains to produce cross-linkable copolymers which formed thermally reversible microspheres (Figure 7).[24]

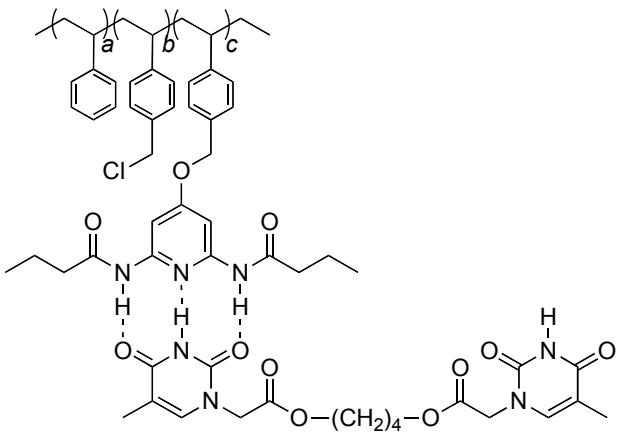

Figure 7. A polystyrene block-copolymer with a diamidopyridine side-chain which can produce thermally reversible microspheres when crosslinked with it's hydrogen-bonding complement.

Bazzi and coworkers showed the synthesis of the first self-complementary triblock copolymer by ROMP (Figure 8).[22] Changing the triblock copolymer sequence produced varied polymer properties, such as the formation of aggregates.[22]

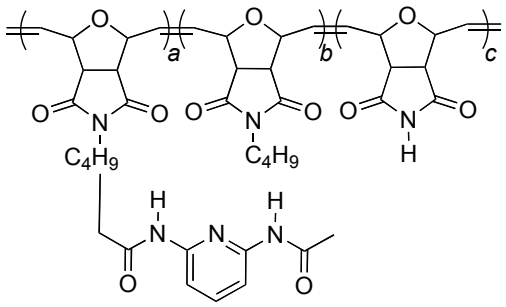

Figure 8. The first self-complementary triblock copolymer system produced *via* ROMP.

Pollino *et al* provided an polymer using ROMP with metal-coordination and hydrogen-bonding side-chains and found that the two sites were orthogonal to one another, thus expanding the side-chain possiblities (Figure 9).[28]

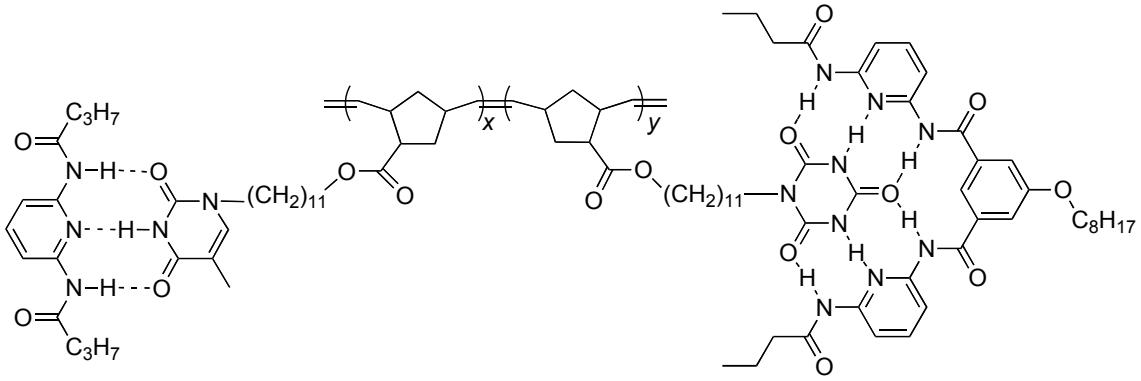

Figure 9. Polynorbornene with orthogonal metal-coordination and hydrogen-bonding side-chains.

Burd *et al* showed combining two competing hydrogen-bonding motifs could create a self-sorting atmosphere further expanding the side-chain library (Figure 10). [23]

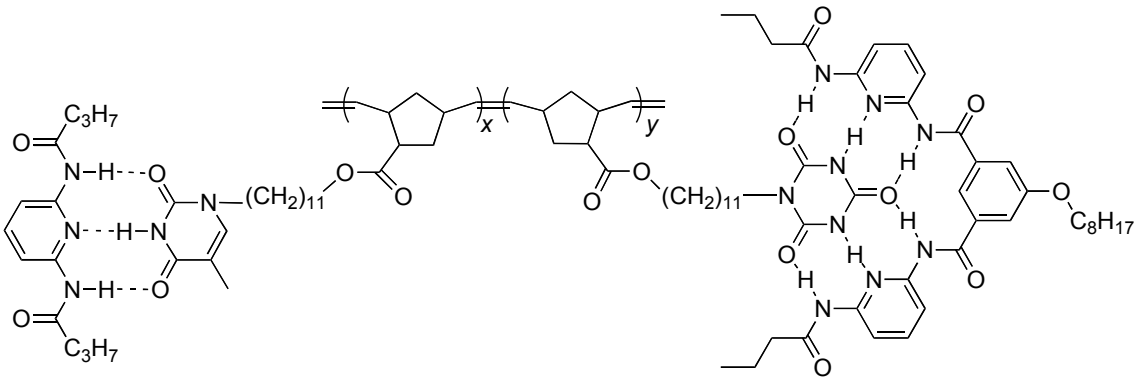

Figure 10. Polymer system with self-sorting side-chain hydrogen-bonding assembly sites.

Although these materials have exhibited an assortment of desired properties, none of these approaches allows for the utilization of sequential self-assembly events on multiple length scales. A first attempt towards the realization of such self-assembly steps, describes the synthesis of block copolymers by utilizing both side- and main-chain molecular recognition sites. To realize the goal of synthesizing AB and ABA type block-copolymers with side-chain sites, a chain-terminator (CT) will be combined with ROMP. The CT is added to a completed polymerization to functionalize one end of a growing polymer chain. These polymers can be combined with their complement telechelic polymer made via the previous CTA route to achieve an ABA type polymer or combined with another CT route terminated polymer for an AB system (Figure 11).

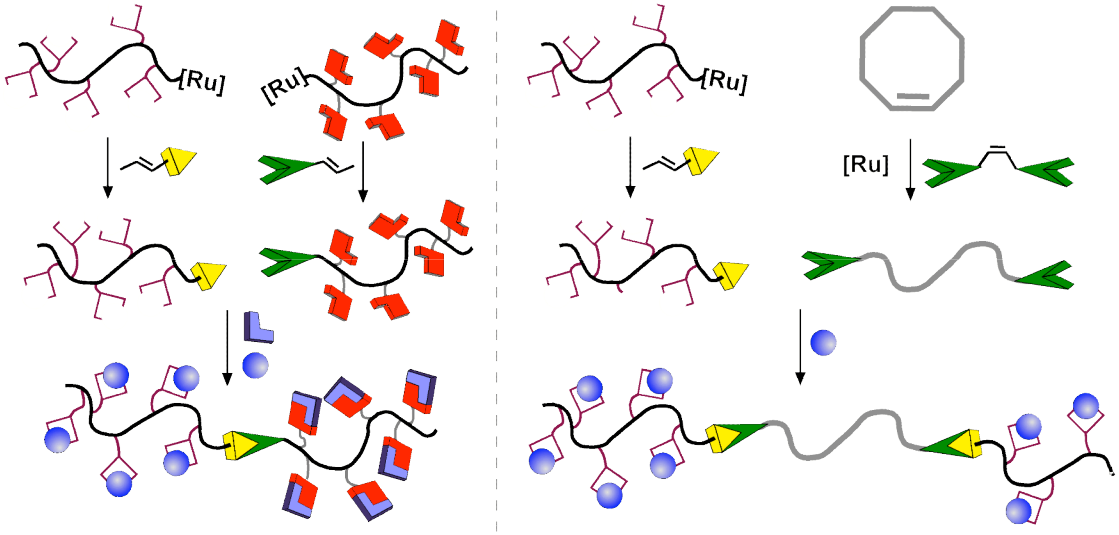

Figure 11. Cartoon depicting the cascade self-assembly strategy towards fully functionalized block copolymers. First, the formation of AB and ABA type block-copolymers via self-assembly, followed by the functionalization of the copolymer side-chains using a second self-assembly step.

CHAPTER 2

SELF-ASSEMBLED BLOCK COPOLYMERS USING TELECHELIC POLYMERS

In this chapter, a strategy for the preparation of copolymers based on the combination of chain-transfer agents (CTAs), ring-opening metathesis polymerization (ROMP), and self-assembly is presented. Ruthenium catalyzed ROMP is a fully functional group tolerant polymerization technique that allows for the facile introduction of virtually any functional group into a polymer main- or side-chain.[17] The inclusion of a functionalized chain-transfer agent (CTA) during the course of ROMP allows for complete polymer end-group functionalization.[17] By employing CTA's containing different functional end-groups such as molecular recognition units, telechelic polymers possessing any desired recognition motif can be synthesized. Additionally, this methodology allows for complete control of the molecular weight of the desired polymer through the control of the CTA to monomer ratio thereby allowing for unprecedented control over end-group functionalization, homo-polymer properties, and ultimately block copolymer properties.[18-21] Following the CTA-based preparation of homopolymers possessing complementary recognition units at the chain termini, rapid self-assembly via exploitation of non-covalent interactions allows for rapid preparation of a large variety of block copolymers.

The design and preparation of the functionalized CTAs must take into consideration two crucial structural components: 1) the type, strength, and behavior of the recognition motifs and 2) the basic structural requirements of the CTA, which must allow for well-defined incorporation to the termini of the homopolymers. To demonstrate the

versatility of this methodology to any non-covalent interaction, recognition units based on either hydrogen-bonding or metal-coordination were investigated. Specifically, palladated sulfur-carbon-sulfur (SCS) pincer ligands, **1**, were employed to explore metal-coordination.[10, 25-34] These metal complexes are known to undergo fast and quantitative self-assembly at room temperature and can accommodate a variety of ligands including functionalized pyridines, nitriles, and phosphines.[10, 25-30, 32, 33, 35] Figure 1 depicts as an example the self-assembled complex formed between a palladated-pincer complex (**1**) and a pyridine unit (**2**). To examine hydrogen-bonding based molecular recognition in the system, diaminopyridines (**3**), known to strongly bind thymine derivatives (**4**) via three hydrogen bonds (K_a = ca. 10^3 M^{-1}), were chosen (Figure 12).[23, 25, 27, 36-42] The basic design of CTAs employed in ROMP requires symmetric, acyclic olefins.[17] Most CTAs reported in the literature are based on *cis*-2-butenediol derivatives.[18-21] However, it was hypothesized that the large terminal recognition units employed in this investigations would be sterically demanding requiring a long alkyl spacer situated between the olefin and recognition unit. Accordingly, a series of novel CTAs (**6-11**) containing nonyl alkyl spacers were chosen as synthetic targets.

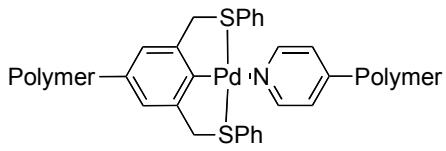

1 **2**

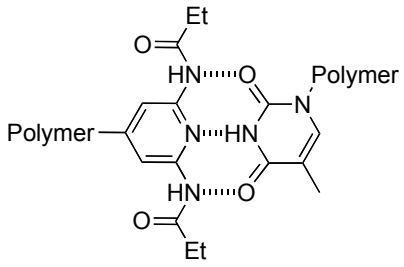

3 **4**

Figure 12. Basic recognition motifs chosen in this study for the self-assembly with metal-coordination, 1 and 2, or hydrogen-bonding, **3** and **4**.

The syntheses of functionalized CTAs **6-11** commences with the preparation of methyl-ester functionalized CTA (**5**) using oxygen assisted Wittig olefination.[43, 44] Subsequent saponification of the ester groups provided diacid **6**, which could be easily functionalized with hydroxy-diaminopyridine (**12**)[45] using a DCC/DMAP esterification protocol to yield hydrogen-bonding CTA **7** (Figure 8). Similarly, pincer ligand functionalized CTA (**8**) was prepared via esterification of **6** using hydroxy-SCS-ligand (**13**), which was subsequently palladated.[46] Reduction of **5** with lithium aluminum hydride gave access to diol **9**, which was then coupled to thymine **14** to give CTA **10**. Condensation of isonicotinoylchloride hydrochloride (**15**) with diol **9** generated pyridine functionalized CTA **11**. The resulting CTAs contain a variety of recognition units ranging from single hydrogen-bonding recognition units (**9** and **11**) to multiple hydrogen-bonding arrays (**7** and **10**) and metal-coordination motifs (**8** and **11**) allowing for rapid tuning of the interaction strengths. Furthermore, **11** can function dually as either a single hydrogen-bonding acceptor or as a ligand for metal-coordination. This versatile library

of CTAs allows for facile, rapid, and modular preparation of self-assembled block copolymers and offers the potential to form multi-block copolymer systems.

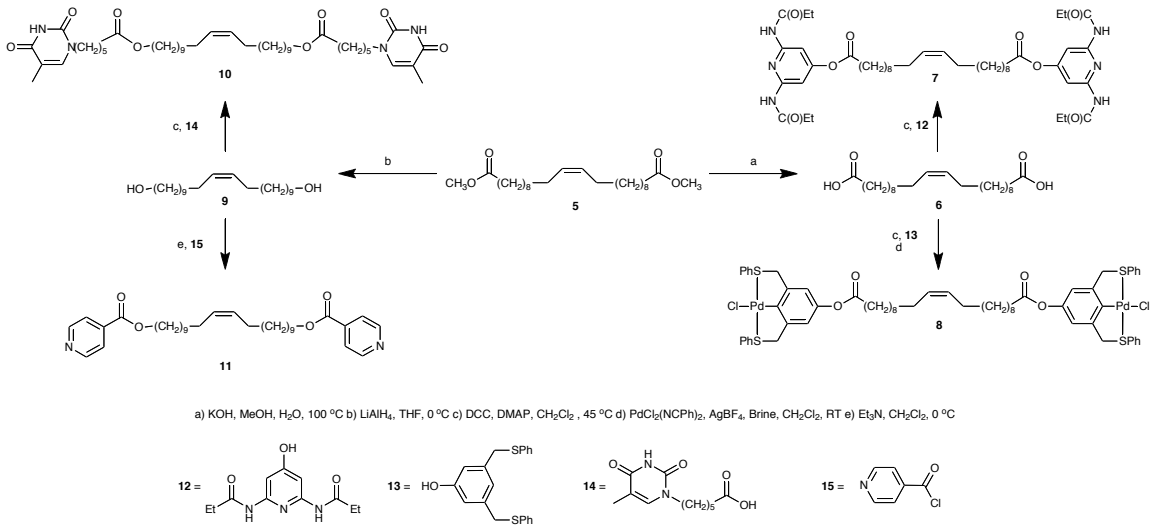

Figure 13. CTA Syntheses.

With the desired CTAs in hand, polymerization experiments were carried out using cyclooctene (**16**) or hexanoic acid cyclooct-4-enyl ester (**17**) as monomer (Figure 14). **17** was formed via the esterification of hexanoic acid with cyclooct-4-enol, which was obtained using a literature procedure.[47] Cyclooctene derivatives were chosen for three distinct reasons: 1) their known ability to polymerize via ROMP, 2) their structural simplicity, which facilitates characterization, and 3) access to a variety of highly functionalized cyclooctene based monomers via asymmetric functionalization of a related compound, cyclooctadiene.[47] Polymerizations were carried out in chloroform using Grubbs' catalysts **18** or **19** in the presence of the desired CTA (**7**, **8**, **10**, or **11**) and monomer (**16** or **17**). All reactions were complete within 72 hours using monomer to catalyst ratios of 4000:1 for **16** and 500:1 for **17** (Figure 14). To investigate if the ratio of

CTA to monomer allows for control over molecular weights, a series of polymers with varying monomer to CTA ratios were synthesized and characterized (Table 1). MALDI of lower molecular weight polymers and GPC analysis of all polymers showed no remaining monomer or CTA demonstrating the successful and quantitative incorporation of the CTA.

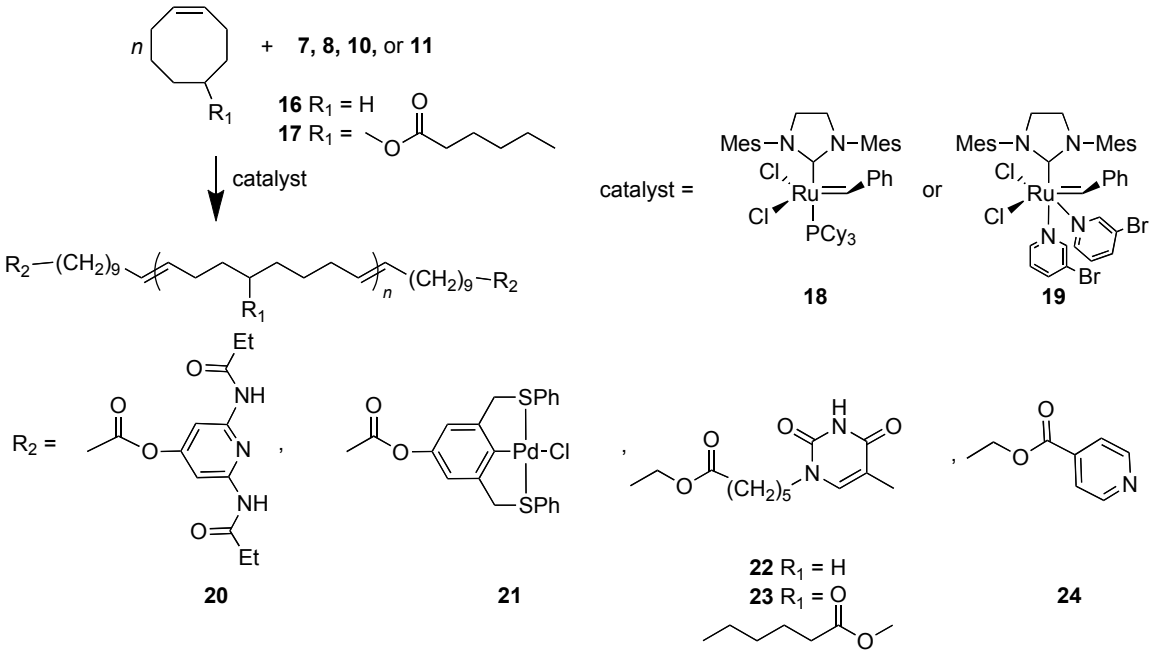

Figure 14. Polymerization of **16** and **17** in the presence of functionalized CTAs.

Table 1. Characterization for the polymerization of 16 or 17 with CTAs 7-11.

CTA	Monomer	[M]/[CTA]	Polymer	Catalyst	M_n (10^{-3})	M_w (10^{-3})	PDI	T_g (°C)
7	**16**	10	**20a**	**18**	5.6 [a] (1.6)[b]	9.1 [a]	1.6	-10
7	**16**	20	**20b**	**18**	8.7 (2.8)	14.8	1.7	-11
7	**16**	50	**20c**	**18**	17.9	32.4	1.8	-15
7	**16**	100	**20d**	**18**	26.4	49.8	1.9	-15
8	**16**	10	**21a**	**19**	6.8 (2.2)	12.8	1.9	-34
8	**16**	20	**21b**	**19**	10.3 (3.2)	15.7	1.5	-35
8	**16**	50	**21c**	**19**	14.7	36.5	2.4	-27
8	**16**	100	**21d**	**19**	49.4	69.5	1.4	-33
10	**16**	10	**22a**	**19**	6.9 (2.1)	13.5	1.9	-23
10	**16**	20	**22b**	**19**	10.8 (3.1)	25.1	2.3	-22
10	**16**	50	**22c**	**19**	15.0	30.8	2.1	-23
10	**16**	100	**22d**	**19**	29.5	48.9	1.6	-22
10	**17**	20	**23b**	**19**	7.5	14.8	2.0	-45
10	**17**	50	**23c**	**19**	12.0	26.5	2.2	-47
10	**17**	100	**23d**	**19**	24.3	37.6	1.6	-57
11	**16**	20	**24b**	**19**	9.0 (2.8)	16.7	1.9	-20
11	**16**	50	**24c**	**19**	36.5	72.5	1.9	-22
11	**16**	100	**24d**	**19**	54.9	90.6	1.7	-22

[a] Determined by gel permeation chromatography in THF relative to monodispersed poly(styrene) standards. [b] Determined by matrix assisted laser desorption/ionization.

As shown in Table 1 and Figure 15, the incorporation of CTAs **7**, **8**, **10**, and **11** allows for a high degree of control over the molecular weights of the final telechelic

polymers through simple variations of the ratio of [Monomer] to [CTA]. For example, Figure 2 shows a plot of M_n (**20**-**24**) as a function of CTA concentration. In all instances, a linear relationship was observed, which clearly demonstrates the ability to tune the molecular weight of the end-functionalized homopolymers independent of the CTA and the recognition motif used.

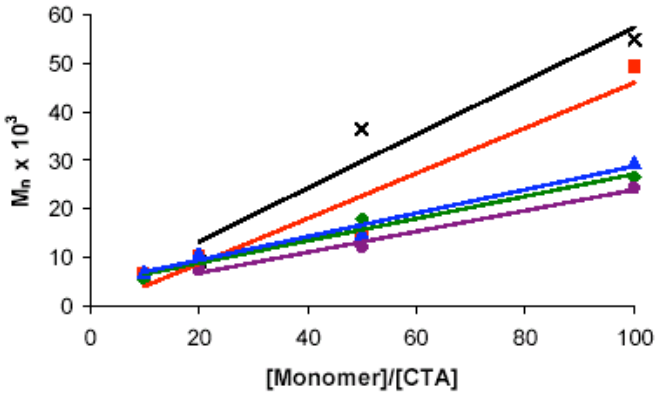

Figure 15. M_n as a function of [Monomer]/[CTA] showing a linear relationship between CTA concentration and molecular weight. Key: Polymers **20** (♦) **21** (■) **22** (▲) **23** (●) **24** (×).

After establishing that cyclooctene (**16**) could be polymerized and end-functionalized with a variety of recognition motifs via a simple and controlled one-step protocol, the self-assembly of the resulting telechelic homopolymers into block copolymers was explored. To demonstrate the modular character of this strategy two different self-assembly strategies were designed and executed. First, homo-block copolymers, the block copolymers are based on two blocks of homopolymers of the same monomer, were directly synthesized via the self-assembly of telechelic homopolymers containing complementary terminal recognition units. Second, telechelic homopolymers were self-assembled into homo-block-copolymers by employment of bisfunctionalized small molecules (**25** and **26**) that possess complementary molecular recognition units

(Figure 16). The second methodology allows for facile formation of non-covalent linkages situated between two homopolymers potentially allowing for the formation of block copolymers possessing short and long segments. The recognition units employed in both studies are identical, which facilitates direct comparison of the two self-assembly strategies. A question that could be answered by comparing these strategies is whether the self-assembly step and the strength of the non-covalent interaction are dependant on the mobility of the complimentary recognition units. If this were the case, one would expect a significant higher bond strength of the non-covalent bond when using the small molecule self-assembly strategy since **25** and **26** are not expected to be diffusion limited as polymer chain ends might be.

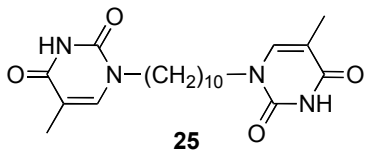

25

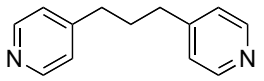

26

Figure 16. Bisfunctionalized small molecules for the self-assembly studies.

Hydrogen bonding-based self-assembly of **20** and **25** or **22** was carried out at room temperature in chloroform and followed *in situ* via ^{1}H-NMR spectroscopy by observing characteristic shifts of the amide signals of **3** as a function of concentration.[48] In the absence of the complementary units, the proton signals of the amides of **20** were observed at 7.8 ppm for a 0.005 M solution. Upon addition of 0.4 equivalents of a 0.010 M solution of **25**, a large downfield shift to 8.4 ppm was observed. To determine the

association constants of the non-covalent interaction, titration experiments were carried out by adding up to 5.2 equivalents of **25**, at 0.4 equivalents per addition, to **20**. The amide signals continued their downfield shift during the titration ending at 10.1 ppm (Figure 17), which is consistent with a K_a of 800 ± 200 [M^{-1}].[49] For the addition of a 0.010 M solution of **22** to a 0.005 M solution of **20**, similar shifts of the amide proton signals were observed with an association constant of 500 ± 100 [M^{-1}]. These binding constant are identical within the error range of the titration experiments demonstrating that the hydrogen bonding-based self-assembly is independent of the self-assembly strategy used and, for the molecular weights studied, not diffusion limited. Furthermore, these association constants are in good agreement with reported K_a values for the system diaminopyridine and thymine[36-41, 48] demonstrating that the formation of block copolymers via hydrogen-bonding is not limited by diffusion or polymer chain interactions (at least for the molecular weights and concentrations studied). Molecular weight determinations via GPC could not be carried out for the hydrogen-bonded block copolymers as it has been suggested that hydrogen-bonded polymers disassociate in the GPC.[28, 30, 48] Therefore, to further explore the hydrogen-bonding self-assembly, flow cell IR measurements were conducted on **20**, **22** and a one to one mixture of the two polymers in $CHCl_3$. The combination showed a new broad stretch at 1696 cm^{-1} after self-assembly due to the carbonyl groups of both **20** and **22** engaging in hydrogen-bonding. The carbonyl group stretches for the pure polymers were found at 1766 cm^{-1} for **20** and 1684 cm^{-1} for **22**. These IR results confirmed further that self-assembly and therefore block-copolymer formation took place.

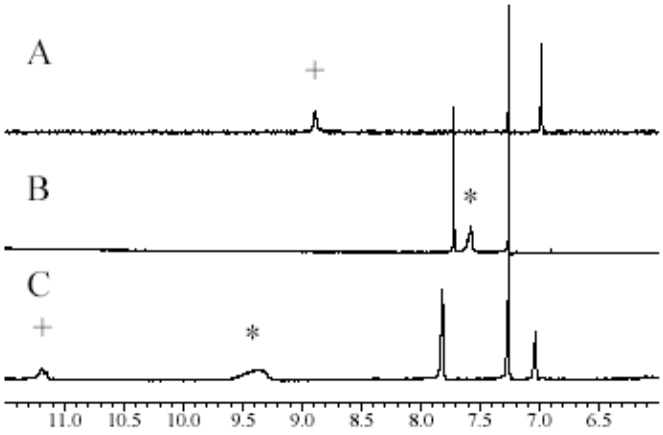

Figure 17. ^{1}H-NMR spectra depicting hydrogen bonding-based self-assembly of **20** with **25**. (A) **25** (+ = imide proton), (B) **20** (* = amide protons), (C) addition of 1.2 equivalents of **25** to **20**.

The block copolymer formation using metal-coordination of **21** was conducted with bisfunctionalized pyridine analog, **26**, or polymer **24**. The experiments were carried out at room temperature using methylene chloride and ^{1}H-NMR was used to follow characteristic shifts which occur during the coordination step.[10, 25-31] One equivalent of the desired pyridine system was added to **21** followed by the addition of one equivalent of $AgBF_4$, which removed the labile chlorine from **21** and allowed metal-coordination between the palladium and the pyridine to occur. Upon coordination, ^{1}H-NMR showed a shift of the aromatic protons of **21** up-field from 7.8 ppm to 7.6 ppm and a characteristic broadening of the signals in the aromatic region.[10, 25-28, 30, 31] Also the characteristic down-field shift of the α-pyridine signal of **26** from 8.5 ppm to 8.0 ppm was observed.[10, 25-28, 30, 31] These characteristic shifts were also observed in the self-assembly of **21** with **24** and clearly indicating that quantitative metal-coordination occurred resulting in block copolymer formation. Furthermore, a GPC experiment was conducted comparing the molecular weight of a physical mixture of the telechelic homopolymers **21** and **24** with the self-assembled block copolymer based on this mixture after metal-coordination. The

molecular weight increased from 9,400 for the physical mixture to 17,000 after metal coordination-based self-assembly. This clearly substantiates the formation of supramolecular block-copolymers using metal-coordination.

To form true block copolymer architectures, similar self-assembly experiments were carried out with homopolymers **20** and **23**, which were formed from monomers **16** and **17,** and possess terminal complementary hydrogen-bonding recognition units. For the ^{1}H-NMR spectroscopy titration experiment, the proton signals of the amides of **20** were initially observed at 7.7 ppm for a 0.006 M solution. Titration experiments were carried out by adding up to 5.6 equivalents of a 0.010 M solution of **23**, at 0.4 equivalents per addition, to **20**. The amide signals continued their downfield shift during the titration ending at 9.7 ppm, which is consistent with a K_a of 400 ± 100 [M^{-1}]. [49] This K_a is within error of the homo-block copolymer system, showing the side-chain of **23** does not limit the block-copolymer formation. A comparable flow cell IR experiment was performed with a one to one mixture of self-assembled **20** and **23** which showed the appearance of a new broad carbonyl stretch at 1709 cm^{-1} which is similar to the carbonyl shift observed in the homo-block system and further confirmed that self-assembly took place.

This chapter demonstrates the formation of a variety of telechelic polymers containing terminal recognition motifs through the incorporation of a novel class of CTAs during the ROMP of cyclooctene derivatives. The resulting telechelic polymers containe terminal functional groups capable of hydrogen-bonding and metal-coordination. The introduction of the molecular recognition units into the polymers was carried out during the polymerization without the need of post-polymerization procedures. This methodology allows for the rapid and facile end-group

functionalization and incorporation of any terminal recognition motif desired in the presence of any functional group in the polymer structure or side-chain. Self-assembly of the telechelic polymers into block copolymer architectures via self-assembly were fast and efficient and substantiated using NMR, IR, MALDI and GPC. This methodology allows for the formation of block copolymers without the need of living polymerization techniques and the incorporation of any recognition unit desired. Further work includes the integration of multiple combinations of non-covalent interactions in one system to form multi-block structures using an orthogonal self-assembly approach.

CHAPTER 3

AB AND ABA TYPE BLOCK COPOLYMERS: COMBINING MAIN AND SIDE-CHAIN SELF-ASSEMBLY

In this chapter, a plan for the combination of main-chain and side-chain self-assembly to create block copolymer architectures is presented. One of the distinct features of DNA is its ability to associate with its complementary partner into a well-defined secondary structure.[50] This property, which has no compare with any synthetic macromolecules, is a result of the location of a well-defined sequence of hydrogen bonding units along the polymer backbone. [50] While DNA has been used as a highly specific building block by a number of groups,[51] the challenges with its synthesis and stability have hindered a more broad use of this molecule. The synthesis of synthetic polymers, which can mimic the specificity of such natural structures, but can be readily accessed in large quantities, is thus a particularly appealing target. To this end, the combination of side-chain and main-chain self-assembly is explored as a preliminary study to mimic DNA and other natural species which create well-defined secondary structures. The architectures presented in this study will be AB and ABA type block copolymers.

The research design is based on side-chain functionalized norbornene monomers that are polymerized via ROMP in the presence of either a functional CT to create a mono end group functionalized polymers or a difuctional CTA for the creation of telechelic or dual end group functionalized polymers. Each monomer as well as CT and CTA contains one (or in the case of the CTA, two) discrete and orthogonal terminal

recognition units. The resulting telechelic polymers can be self-assembled into block copolymers quickly and efficiently, and this assembly can be preceded or followed by the addition of a second self-assembly step to functionalize the polymers through basic molecular recognition events along the side-chain of the functional polymer.

In order to realize the sequential molecular recognition strategy towards functionalized block copolymers, monomers **27** and **28** were utilized which contain a terminal hydrogen-bonding recognition unit (**27**) or a terminal metal-coordination site (**28**) (Figure 18). Both monomers contain three important features 1) a norbornene which is known to undergo ROMP quickly, efficiently, and often under living conditions 2) a spacer unit which allows the self-assembly motif to be isolated from the backbone after polymerization and 3) the molecular recognition group that will undergo the selective self-assembly. The hydrogen bonding moiety on **27** is a guanine derivative that has a DDA hydrogen-bonding motif while the recognition unit on **28** is a paladated SCS pincer complex which has been shown to form assemblies with pyridine, phosphine and nitrile derivatives.[10, 25-34] The complimentary recognition units for **27** and **28** employed in this study are the cytosine derivative **29** and pyridine (**30**). The hydrogen-bonding between guanine and cytosine has an association constant of approximately 10^4 M^{-1} in $CDCl_3$,[40] while the metal-coordination system of **28** and **30** have been shown to form strong and easily characterizable assemblies in a variety of solvents.[10, 25-33]

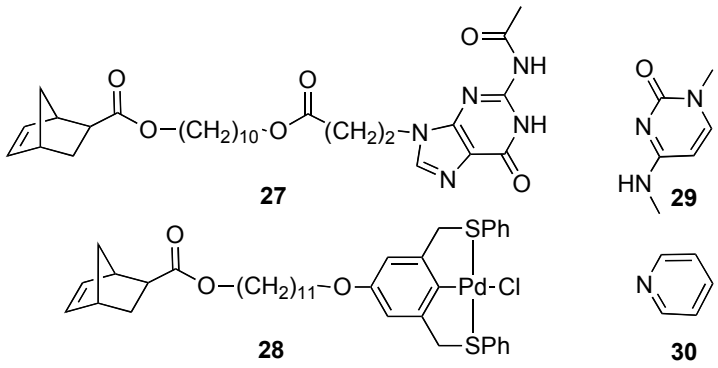

Figure 18. Norbornene based monomers **27** and **28** with functional groups for side-chain self-assembly and their complementary recognition motifs **29** and **30**.

The CTs that will transfer their functional group to one end of the main-chain of the norbornene polymers are based on bis-isophthalamide (**31**) and cyanuric acid (**32**) while CTA **33**, which will provide self-assembly motifs to both end-groups of the telechelic polymer, is also based on bis-isophthalamide (Figure 19). The self-assembly between bis-isophthalamide and cyanuric acid is known to form strong hydrogen bonds with association constants in polymeric system around 10^4 M^{-1} in $CDCl_3$,[9, 11, 52, Burd, 2005 #3] making this the recognition pair of choice for the formation of the main-chain supramolecular polymer self-assembly.

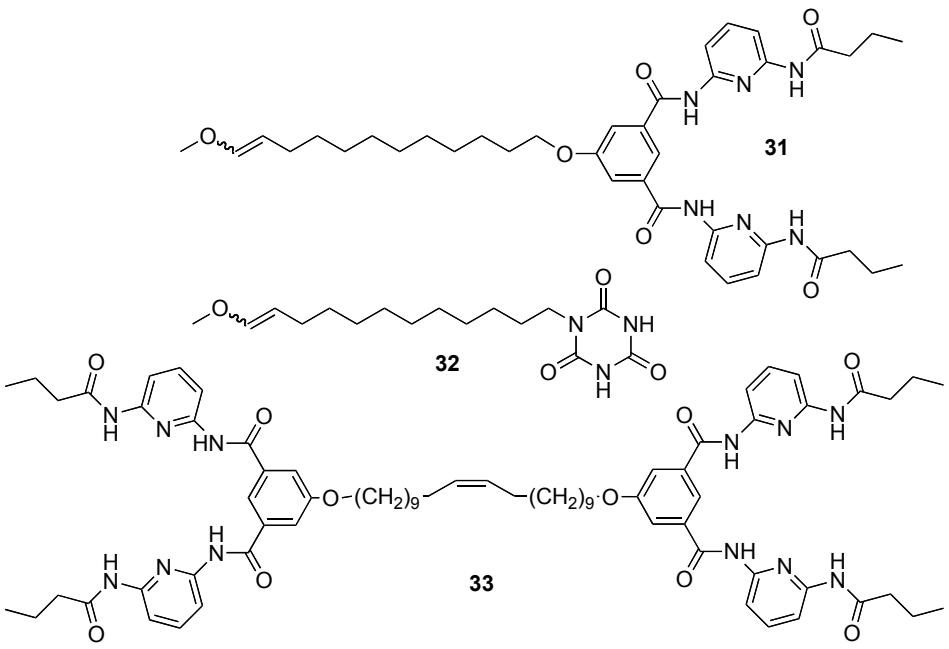

Figure 19. End-functionalized CTs **31** and **32** and difuntional CTA **33**.

Monomers **27** and **28**, CTs **31** and **32**, and CTA **33** were synthesized either as reported in the literature or in close analogy to literature procedures. With the functionalized monomers, CTs and CTA in hand, the polymerizations were carried out to synthesize the building blocks for the block copolymer study based on sequential molecular recognition self-assembly steps. The polymerizations of the monomers were carried to completion using **34** in CH_2Cl_2 with a monomer to catalyst ratio of 10 to 1. The polymerizations were terminated by the addition of the desired CT which removes the ruthenium catalyst from the polymer and replaces it with the functional portion of the CT resulting in the formation of single end-group functionalized polymers containing a terminal recognition motif and ruthenium complex **39**. The synthesis of polymer **37** is shown in Figure 19 as an example. Telechelic polymers based on **27** with **31** and **28** and **32** were synthesized.

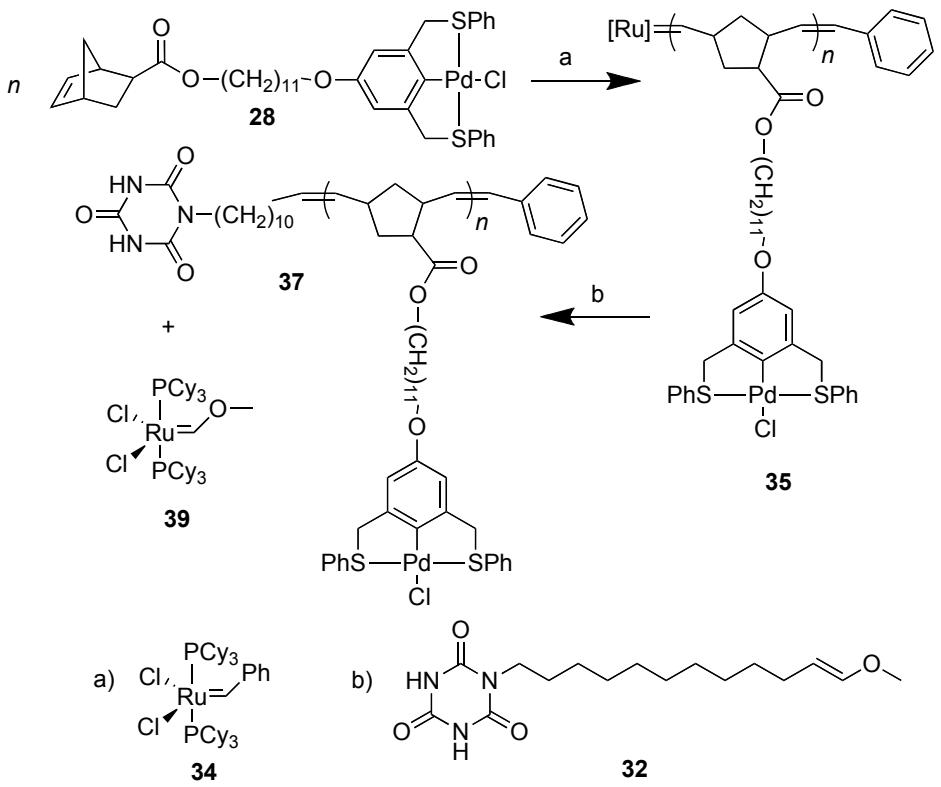

Figure 20. Addition of **32** to the completed homopolymer **35** forming the Fischer carbene (**39**) and the end-functionalized homopolymer (**37**).

To synthesize the two end-functionalized (or telechelic) polymer, cyclooctene was polymerized in the presence of **33** as described in the literature. Polymers **36 - 38** were characterized by NMR, GPC, and MALDI TOF. The characterization data of all polymers are shown in Table 2.

Table 2. Characterization of Polymers 36 - 38

Monomer	CT/CTA	Polymer	M_n (10^{-3})	M_w (10^{-3})	PDI
27	**31**	**36**	2.6[a] (5.3)[b]	3.4[a]	1.3
28	**32**	**37**	1.3[a] (7.9)[b]	2.0[a]	1.5
Cyclooctene	**33**	**38**	15.4[c] (2.9)[b]	19.0[c]	1.2

[a] Determined by gel-permeation chromatography in CH_2Cl_2 relative to monodispersed poly(styrene) standards performed using a Waters 1525 binary pump coupled with a Waters 2414 refractive index detector. [b] Determined by matrix assisted laser desorption/ionization. [c] Determined by gel-permeation chromatography in CH_2Cl_2 relative to monodispersed poly(styrene) standards performed using a Shimadzu 10A.

A detailed study of the competitive nature of the hydrogen-bonding systems is required to assess all self-assemblies. A series of ^{1}H-NMR experiments were conducted to ascertain the orthogonal nature of the self-assembly motifs and to determine the K_d and/or K_a values of each hydrogen bonding recognition pair. These findings are summarized in Table 3. In each case a 0.005 M solution in $CDCl_3$ of species A was titrated with 0.1 mL of a 0.010 M solution in $CDCl_3$ of species B. Characteristic signals in the ^{1}H-NMR spectrum of A were monitored for changes upon the addition of B and were analyzed using Chem-Equili to determine K_d or K_a values. The K_d for **Poly-27** and for recognition motif **29** were found to be less than 1 in both cases. Therefore, the dimerization of the hydrogen-bonding self-assembly sites will not effect the overall block copolymer formation nor side-chain self-assembly. Furthermore, the K_a of CTs **31** and **32** into **29** or **27** were also found to be less than 1. These results demonstrate that the investigated hydrogen-bonding pairs are orthogonal to each other, i.e. the individual recognition pairs self-sort.

Table 3. Association constants for competitive binding

Species A	Species B	K_d [M^{-1}]	Species A	Species B	K_a [M^{-1}]
27	**27**	5 ± 1	**27**	**31**	< 1
Poly-27	**Poly-27**	< 1	**27**	**32**	< 1
29	**29**	< 1	**Poly-1**	**27**	3 ± 1
			29	**31**	< 1
			29	**32**	< 1

The first block copolymer system to be studied was the ABA type triblock copolymer which is based on the self-assembly via hydrogen bonding of polymers **37** and **38** followed by the side-chain functionalization of **37** with **30**. The block copolymer formation was studied in detail using ^{1}H-NMR spectroscopy. During the ^{1}H-NMR experiment a 0.010 M solution of either **37** or the assembly of **37•30** in $CDCl_3$ was titrated into a 0.005 M $CDCl_3$ solution of **38** and the imide signals of the bis-isophthalamide end-groups of **38** were monitored. During the titration experiment, the imide signals were found to shift from 8.8 ppm to about 13.2 ppm after the addition of 4.8 equivalents of the titrate which corresponds to a K_a of 2.83 x 10^3 ± 500 M^{-1}. After block copolymer formation, **30** was coordinated onto the side-chains of **37**. The reverse self-assembly strategy was also studied: the coordination of **30** onto **37** followed by the addition of **38**, i.e. first the polymer side-chain was functionalized followed by the formation of the triblock copolymer. In this case, the K_a of the main-chain self-assembly event was found to be 2.69 x 10^3 ± 400 M^{-1}. It is important to note that both K_a values are the same when including the error demonstrating that the functionalization of the side-chain before or after backbone self-assembly has no effect on the K_a of the backbone and therefore on the assembly of the block copolymer. The functionalization of the side-

chains was monitored by diagnostic shifts in the ^{1}H-NMR of the SCS pincer side-chain of **37** and of **30**. For coordination to occur between **37** and **30**, a one to one mixture of the two species was combined and one equivalent of $AgBF_4$ was added to the mixture. The $AgBF_4$ removes the labile chlorine from **37** and allows **30** to immediately coordinate to the palladium. The ^{1}H-NMR after the addition of $AgBF_4$ shows a diagnostic upfield shits of the protons on the pincer ligand from 7.8 ppm to 7.6 ppm and of the α-pyridine proton signals shift from 8.5 ppm to 8.1 ppm. These shifts were identical for the ABA block system regardless if the coordination step was carried out before or after the backbone formation. In both cases the assembly was quantitative and immediate.

Table 4. Association Constants for the ABA Self-Assembly System in $CDCl_3$.

First Assembly	Second Assembly	K_a [M^{-1}]
37•38	**(37•38)•30**	$2.83 \times 10^3 \pm 500$
37•30	**(37•30)•38**	$2.69 \times 10^3 \pm 400$

The AB block copolymer system was studied in close analogy to the ABA system using ^{1}H-NMR spectroscopy. There are five distinct combinations of polymers **36** and **37** and their complement side-chain recognition units **29** and **30**. The results for the K_a of hydrogen-bonding events of the side-chains and the main-chains for each of the five pathways are summarized in Table 5.

For the titration experiments for the block copolymer formations, i.e. the main-chain self-assembly steps, the molarities of the solutions of the titrants were doubled to prevent the use of large volumes. 0.010 M for the titrant and 0.020 M for the solution being added were used and the amount of the species being added was decreased to

aliquots of 0.05 mL. For each pathway of the AB system, the imide signals of the bis-isophthalamide end-groups of **36** were monitored for any change upon the addition of **37** to yield the K_a for the main-chain hydrogen bonding step. To determine the K_a of the side-chain assembly of **36** with **29**, the imide signals of the guanine side-chain were monitored for change during addition of **29**. The side-chain functionalization via the metal-coordination of polymer **37** with **30** was characterized as described above for the ABA triblock copolymer.

The five distinct self-assembly pathways are: (A) the hydrogen-bonding based self-assembly of the AB backbone formed by combining **36** and **37** followed by hydrogen-bonding based side-chain functionalization with **29**, and finally the side-chain functionalization via the metal-coordination with **30**. (B) The second pathway studied the formation of backbone **36•37**, followed by metal-coordination with **30** and thirdly the side-chain functionalization with **29**. (C) The third pathway examined the side-chain hydrogen-bonding functionalization first, followed by the block copolymer formation and then the metal-coordination functionalization of the side-chain of one polymer block. (D) In the fourth pathway, the side-chains of the homopolymers **36** and **37** are assembled first and then the block copolymer is formed via self-assembly. (E) For the final pathway the quantitative self-assembly of metal-coordinated homopolymer **37•30** was titrated into polymer **36** to form the block copolymer followed by side-chain functionalization with **29**.

The detailed ^{1}H-NMR titration studies yielded important insights into the system. Comparing the first two pathways it was found that the coordination of **37** with **30** to be quantitative for both systems and the same strength (K_a values) for the side-chain

functionalization step (K_a = 750 x 10^2 ± 80 M^{-1} for the first pathway and 700 x 10^2 ± 100 M^{-1} for the second one). These results demonstrate that the side-chain functionalization steps do not interfere with each other in the presence of the diblock copolymer. When analyzing the third pathway, a K_a of 790 x 10^2 ± 60 M^{-1} was measured for the side-chain functionalization and a K_a of 2.58 x 10^3 ± 800 M^{-1} for the diblock formation. The hydrogen bond strengths are comparative to the previous pathways. In the fourth pathway the K_a of the side-chain functionalization and diblock formation were measured to be 790 x 10^2 ± 60 M^{-1} and 2.64 x 10^3 ± 700 M^{-1} which is comparable to pathways 1-3. For the final pathway the K_a of the block copolymer formation was 2.53 x 10^3 ± 500 M^{-1} and the K_a of the side-chain functionalization was found to be 750 x 10^2 ± 120 M^{-1}. For all pathways, quantitative metal-coordination was observed. Overall the study of the AB block copolymer system showed that the diblock copolymer formation is independent of any side-chain functionalization and can be carried out before or after the functionalization step. The same holds true for the hydrogen bonding based and metal-coordination based side-chain functionalization steps.

Table 5. Association Constants for the AB Self-Assembly System in $CDCl_3$.

First Assembly	Second Assembly	Third Assembly	K_a [M^{-1}] of side-chain	K_a [M^{-1}] of backbone
36•37	**(36•37)•29**	**((36•37)•29))•30**	750 x 10^2 ± 80	2.70 x 10^3 ± 600
36•37	**(36•37)•30**	**((36•37)•30))•29**	700 x 10^2 ± 100	2.70 x 10^3 ± 600
36•29	**(36•29)•37**	**((36•29)•37))•30**	790 x 10^2 ± 60	2.58 x 10^3 ± 800
36•29	**37•30**	**(36•29)(37•30)**	790 x 10^2 ± 60	2.64 x 10^3 ± 700
37•30	**(37•30)•36**	**((37•30)•36))•29**	750 x 10^2 ± 120	2.53 x 10^3 ± 500

The next study involved using Differential Scanning Calorimetry (DSC) to determine the T_g for both the homopolymers and the main-chain AB and ABA self-assembled systems. For homopolymers **36**, **37** and **38**, the T_g's were found to be 47 °C, 26 °C and –15 °C respectively. In the AB system two T_gs for **37•38** were found at 23 °C and –18 °C demonstrating behavior of a blcok copolymer system. The same is true for the ABA system combining **36** and **37** to yield T_gs present at 49 °C and 25 °C.

In conclusion, this chapter demonstrates preliminary studies of a sequential multi-site recognition event combining side- and main-chain self-assemblies. This system exhibits self-assembly on multiple length scales allowing us to move closer to mimicking nature's complexity. To achieve this goal, homopolymers containing one or two functional end-group(s) were synthesized by ROMP through the addition of a functional CT or CTA. These homopolymers were combined in a variety of pathways to form AB and ABA type block copolymers containing functionalized side-chains. The orthogonal nature of all side- and main-chain self-assembly events was investigated by ^{1}H-NMR spectroscopy and DSC experiments. The AB and ABA systems were found to assemble with K_a within error of one another regardless of pathway and acted as block copolymer systems when characterized via DSC.

CHAPTER 4
CONCLUSIONS AND FUTURE WORK

The formation of block copolymers via main-chain self-assembly was realized in a variety of pathways and yielded different possible architectures while incorporating several distinct and orthogonal self-assembly motifs. These self-assembled block copolymer were characterized with ^{1}H-NMR, IR, and mass spectroscopy, as well as GPC and DSC experiments. The novel method for forming telechelic polymers with a CTA was well-studied and was the first published example of this homopolymer synthesis. In the case of using CTs for synthesizing polymers with one end-group these results are preliminary and future studies will be conducted.

APPENDIX A

EXPERIEMENTAL

General methods: All reagents were purchased either from Acros Organic, TCI or Aldrich. All chemicals were reagent grade and used without further purification. Et_3N, $CHCl_3$, and cyclooctene were distilled from CaH_2. CH_2Cl_2 was dried via passage through Cu_2O and alumina columns and THF was dried by passage through alumina columns. NMR spectra were recorded on a Varian Mercury spectrometer (300 MHz). Chemical shifts are reported in parts per million (ppm), using residual solvent as an internal standard. Data are reported as follows: chemical shift, multiplicity (s = singlet, d = doublet, t = triplet, q = quartet, dd = doublet of doublets, m = multiplet, b = broad), coupling constant and integration. Mass spectral analysis was provided by the Georgia Tech Mass Spectrometry Facility. Elemental analyses were conducted at Atlantic Microlab, Inc.

The synthesis of 10-hydroxydecyl bicyclo[2.2.1]hept-5-ene-2-carboxylate,[26] 5-hydroxy-*N*1,*N*3-bis(6-propionamidopyridin-2-yl)isophthalamide,[23]monomer **28**[46] and recognition unit **29**[53] have been published elsewhere.

***cis*-Docos-11-enedioic acid (6):** A solution of **5** (2.46 g, 6.17 mmol) in a mixture of MeOH/H_2O (1 to 1: 20 mL) was stirred with KOH (0.70 g) for six hours. The solution was poured into 1N HCl (50 mL) and extracted with CH_2Cl_2 (100 mL). The organic layer was collected, dried ($MgSO_4$), and the solvent removed to yield **6** as a white powder (70% yield). ^{1}H-NMR (300 MHz, $CDCl_3$) δ = 1.27 (mb, 24H), 1.63 (t, *J* = 7.1 Hz, 4H),

1.99 (t, *J* = 5.5 Hz, 4H), 2.33 (t, *J* = 7.7 Hz , 4H), 5.36 (dd, *J* = 4.4, 6.7 Hz, 2H), 11.66 (sb, 2H) ^{13}C NMR (300 MHz, $CDCl_3$) δ = 25.0, 27.5, 29.9, 30.1, 32.9, 34.5, 53.7, 128.7, 130.0, 134.0, 180.7 MS (ESI): *m/z* (%) = 368.3 (M^+ calculated 368.29) Elemental Analysis calculated for $C_{22}H_{40}O_4$: C 71.70, H 10.94, found: C, 71.95, H, 10.81

***cis*-Docos-11-enedioic acid bis-(2,6-bis-propionylamino-pyridin-4-yl) ester (7):** Compound **6** (0.322 g, 0.841 mmol) was dissolved in CH_2Cl_2 (20 mL) and combined with dicyclohexylcarbodiimide (0.433 g), *N,N*-dimethylaminopyridine (11.1 mg) and **12** (0.524 g). The solution was heated to reflux for 16 hours and then cooled to room temperature. The solid was filtered off and the filtrate was purified using column chromatography (silica, ethyl acetate: CH_2Cl_2 2:1) to yield **7** as a white solid in 63% yield. ^{1}H-NMR (300 MHz, DMSO-d_6) δ = 1.02 (t, *J* = 7.1 Hz, 12H), 1.24 (mb, 24H), 1.59 (t, *J* = 6.0 Hz, 4H), 1.96 (t, *J* = 5.5 Hz, 4H), 2.39 (q, *J* =7.7, 7.1 Hz, 8H), 2.57 (t, *J* = 7.1 Hz, 4H), 5.30 (dd, *J* = 4.4, 5.0 Hz, 2H), 7.53 (s, 4H), 10.16 (s, 4H) ^{13}C NMR (300 MHz, $CDCl_3$) δ = 9.5, 24.9, 25.3, 25.8, 26.6, 27.5, 30.5, 31.3, 33.0, 34.4, 35.2, 56.0, 103.7, 130.0, 151.3, 161.3, 173.2 MS (ESI): *m/z* (%) = 806.6 (M^+ calculated 806.49) Elemental Analysis calculated for $C_{44}H_{66}N_6O_8$: C 65.48, H 8.24, N 10.41, found: C 62.65, H 8.11, N 9.56

***cis*-Docos-11-enedioic acid bis-(Pd-Cl-{3,5-Bis[(phenylsulfanyl)methyl]phenoxy}) ester complex (8):** Compound **6** (0.403 g, 1.052 mmol) was dissolved in CH_2Cl_2 (20 mL) and combined with dicyclohexylcarboimide (0.543 g), *N,N*-dimethylaminopyridine (32 mg) and **13** (0.891 g). The solution was heated to reflux for 16 hours and then

cooled to room temperature. The solid was filtered off and the filtrate was purified using column chromatography (CH_2Cl_2, silica) to yield *cis*-docos-11-enedioic acid bis-(3,5-bis-phenylsulfanylmethyl-phenyl) ester (0.977 g, 0.968 mmoles) as an orange solid. This ester was then combined with $PdCl_2(NCPh)_2$ (0.817 g) in a 1 to 1 mixture of CH_2Cl_2 (20 mL) and CH_3CN (20 mL) and stirred at room temperature for 45 minutes, then $AgBF_4$ (0.754 g) was added and stirred for 45 additional minutes. Finally, brine (180 mL) was added and stirred for 18 hours. The organic layer was collected and the solvent removed. The product was purified using column chromatographgy (silica, a) CH_2Cl_2 b) CH_2Cl_2:MeOH 98:2) to obtain **8** as an orange product in 47% yield. ^{1}H-NMR (300 MHz, $CDCl_3$) δ = 1.26 (mb, 24H), 1.69 (t, J = 6.6 Hz, 4H), 1.97 (t, J = 6.6 Hz, 4H), 2.47(t, J = 7.1 Hz, 4H), 4.57 (s, 8H), 5.33 (dd, J = 5.5 Hz, 2H), 6.74 (s, 4H), 7.38 (m, 12H), 7.84 (m, 8H) ^{13}C NMR (300 MHz, $CDCl_3$) δ = 10.1, 25.3, 27.6, 30.1, 33.3, 34.4, 34.7, 52.0, 115.8, 129.3, 129.9, 130.2, 131.7, 132.3, 135.8, 136.7, 137.6, 137.9, 139.6, 150.3 MS (ESI): *m/z* (%) = 1253.8 (M^+ calculated-Cl 1253.2) Elemental Analysis calculated for $C_{62}H_{70}Cl_2O_4Pd_2S_4$: C 57.67, H 5.46, found: C 57.35, H 5.93

***cis*-Docos-11-ene-1,22-diol (9):** A solution of **5** (3.45 g, 8.65 mmol) was combined with $LiAlH_4$ (2 eq) in THF (50 mL) at 0 °C and stirred for 18 hours. Water (100 mL) was added to the reaction and the solution was extracted with CH_2Cl_2 (2 x 50 mL). The organic layer was collected, dried, and removed to yield **9** as a white powder (98%). ^{1}H-NMR (300 MHz, $CDCl_3$) δ = 1.28 (mb, 34H), 2.00 (t, J = 7.1 Hz, 4H), 3.63 (t, J = 6.6 Hz, 4H), 5.34 (dd, J = 6.6 Hz, 2H) ^{13}C NMR (300 MHz, $CDCl_3$) δ = 26.1, 27.5, 29.5, 29.6, 29.7, 29.9, 30.1, 32.9, 33.1, 63.4, 130.1

***cis*-1,22-di-6-(5-Methyl-2,4-dioxo-3,4-dihydro-2H-pyrimidin-1-yl)-hexanoic acid-docos-11-enyl ester (10):** Compound **14** (1.750 g, 7.285 mmol) was combined with **9** (0.910 g, 2.91 mmol) in CH_2Cl_2 with dicyclohexylcarboimide (1.503 g) and *N,N*-dimethylaminopyridine (89 mg) and heated to 45 °C. The reaction was complete after 48 hours yielding a yellow mixture of products which were separated using column chromatography (silica, ethyl acetate). **10** was collected as a pale yellow solid (72%). ^{1}H-NMR (300 MHz, DMSO-d_6) δ = 1.20 (mb, 28H), 1.52 (m, *J* = 7.1 Hz, 4H), 1.66 (mb, 4H), 1.73 (d, *J* = 2.2 Hz, 6H), 1.97 (t, *J* = 3.9 Hz, 4H), 2.26 (t, *J* = 7.1 Hz, 4H), 3.16 (t, *J* = 5.0 Hz, 4H), 3.57 (t, *J* = 6.6 Hz, 4H), 3.97 (t, *J* = 6.6 Hz, 4H), 5.38 (dd, *J* = 4.9 Hz, 2H), 7.52 (s, 2H), 11.18 (s, 2H). ^{13}C NMR (300 MHz, $CDCl_3$) δ = 12.7, 24.7, 25.0, 25.1, 25.7, 25.8, 26.2, 26.6, 27.5, 28.9, 30.1, 31.3, 33.1, 34.3, 48.6, 64.9, 110.8, 130.0, 140.7, 150.9, 164.4, 173.6 MS (ESI): *m/z* (%) = 784.5 (M^+ calculated 784.54) Elemental Analysis calculated for $C_{44}H_{72}N_4O_8$: C 67.32, H 9.24, N 7.14, found: C 65.76, H 9.29, N 7.74

***cis*-1,22-Diisonicotinic acid-docos-11-enyl ester (11):** In dry CH_2Cl_2 (20 mL), **9** (0.400 g, 1.28 mmoles) was combined with **15** (0.682 g) and Et_3N (0.45 mL) and stirred at room temperature for 18 hours. The mixture was washed with 1 N HCl, 2M NaOH, and brine, and then dried to yield the product as a white powder in 93% yield. ^{1}H-NMR (300 MHz, $CDCl_3$) δ = 1.28 (mb, 24H), 1.79 (t, *J* = 7.7 Hz, 4H), 1.99 (t, *J* = 5.5 Hz, 4H), 3.63 (t, *J* = 6.6 Hz, 4H), 4.40 (t, *J* = 6.6 Hz, 4H), 5.32 (dd, *J* = 5.0 Hz, 2H), 8.18 (d, *J* = 4.9 Hz, 4H), 8.90 (s, 4H) ^{13}C NMR (300 MHz, $CDCl_3$) δ = 26.3, 26.6, 27.3, 27.6, 28.9, 29.5, 30.1,

33.1, 34.3, 67.3, 125.1, 130.0, 142.1, 146.2, 163.4 MS (ESI): *m/z* (%) = 550.4 (M^+ calculated 550.38). Elemental Analysis calculated for $C_{34}H_{50}N_2O_4$: C 74.14, H 9.15, N 5.09, found: C 68.81, H 9.24, N 4.00

6-(5-Methyl-2,4-dioxo-3,4-dihydro-2H-pyrimidin-1-yl)-hexanoic acid (14): 6-Bromo hexanoic acid (3.946 g) was heated to 75 ºC in MeOH (30 mL) with a catalytic amount of H_2SO_4 (1 mL) for 16 hours. 6-Bromohexanoic acid methyl ester (2.696 g, 64%) was distilled from the system and combined with thymine (4.878 g), K_2CO_3 (1.932 g), and NaI (1.932 g) in dry DMSO (30 mL). The solution was heated to 90 ºC for four hours. The solution was acidified with 1N HCl and extracted with CH_2Cl_2 (100 mL). The organic layer was collected and removed to yield 6-(5-methyl-2,4-dioxo-3,4-dihydro-2H-pyrimidin-1-yl)-hexanoic acid methyl ester (2.529 g, 77%). The thymine ester was heated to 95 ºC in a mixture of H_2O/MeOH (1 to 1, 50 mL) with KOH (1.526 g) for 16 hours. The solution was poured into 1 N HCL (100 mL) and extracted with CH_2Cl_2 (100 mL). The organic layer was collected and removed to yield **14** as a white powder (97%, 48% overall yield).

^{1}H-NMR (300 MHz, DMSO-d_6) δ = 1.22 (m, *J* = 6.6 Hz, 2H), 1.50 (mb, *J* = 7.7 Hz, 4H), 1.72 (d, *J* = 7.1 Hz, 3H), 2.20 (t, *J* = 7.1 Hz, 2H), 3.55 (t, *J* = 7.1 Hz, 2H), 7.52 (s, 1H), 11.18 (s, 1H), 11.99 (s, 1H) ^{13}C NMR (300 MHz, DMSO-d_6) δ = 12.7, 24.9, 26.1, 29.0, 34.3, 47.7, 109.0, 142.1, 151.4, 164.9, 174.9. MS (ESI): *m/z* (%) = 241.1 (M^+ calculated 241.11).

9-(3-(2-Acetamido-6-oxo-1H-purin-9(6H)-yl)propanoyloxy)nonyl bicyclo[2.2.1]hept-5-ene-2-carboxylate (27): A solution of 10-hydroxydecyl bicyclo[2.2.1]hept-5-ene-2-carboxylate (0.446g, 1.51 mmol) and Et_3N (3.7 mL) were combined in $CHCl_3$ (100 mL) and cooled to 0 ºC. Acryol chloride (1.23 mL, 15.1 mmol) was added slowly, and the reaction was allowed to stir overnight. The solution was poured into MeOH (200 mL) and the solid was filtered. The organic layer was removed and the solid purified by column chromoatography (silica hexane/ethyl acetate 3 to 1) to provide 10-(acryloyloxy)decyl bicyclo[2.2.1]hept-5-ene-2-carboxylate as a white solid (20% yield). 10-(acryloyloxy)decyl bicyclo[2.2.1]hept-5-ene-2-carboxylate (0.100 g, 0.287 mmol) was dissolved in DMSO (25 mL). N-(6-Oxo-6,9-dihydro-1H-purin-2-yl)-acetamide (0.554g, 2.87mmol) was added followed by a catalytic amount of t-BuOK (0.3 mL, 1.0 M solution in THF). The solution was heated to 60 ºC and stirred for 24 hours. The DMSO was removed via vacuum at 60 ºC and ethyl acetate was added (50 mL). The solid was filtered and the organic layer was removed. The resulting solid was purified by column chromatography (THF:hexane 4 to 1) to yield a white solid (0.108 g, 70% yield). ^{1}H-NMR (300 MHz, $CDCl_3$) d = 1.37 (mb, 15H), 1.57 (m, 5H), 1.91 (m, 1H), 2.21 (m, 1 H), 2.36 (s, 3H), 2.83 (t, 2H), 2.92 (m, 1 H), 3.03 (m, 1 H), 3.63 (t, 2H), 4.07 (t, 2H), 4.31 (t, 2H), 6.12 (m, 2H), 7.74 (s, 1H), 8.67 (s, 1H), 11.97 (s, 1H). ^{13}C NMR (300 MHz, $CDCl_3$) d = 24.4, 25.9, 26.0, 28.6, 28.7, 28.8, 29.2, 29.5, 30.5, 34.3, 41.7, 43.2, 46.6, 46.7, 63.2, 64.9, 120.7, 136.3, 138.5, 140.5, 148.3, 149.3, 155.5, 171.1, 174.2, 175.8. MS (ESI): m/z (%) = 542.4 (542.3 M+ calculated). Elemental Analysis calculated for $C_{27}H_{37}N_5O_6$: C 61.46, H 7.07, N 13.27, found: C 61.48, H 7.09, N 13.31

5-(12-Methoxydodec-11-enyloxy)-*N*1,*N*3-bis(6-propionamidopyridin-2-yl)isophthalamide (31): 12-Bromo-1-methoxydodec-1-ene (0.150 g, 0.541 mmol) and 5-hydroxy-*N1,N3*-bis(6-propionamidopyridin-2-yl)isophthalamide (0.299 g, 0.595 mmol), were combined in DMSO (30 mL) with K_2CO_3 (0.082 g, 0.60 mmol). The mixture was heated to 60 ºC and stirred under argon for 24 hours. H_2O (30 mL) was added to the solution which was then extracted with CH_2Cl_2. The organic layer was washed with 1 N HCl (30 mL) and brine. The organic layer was removed and the solid was purified by column chromatography (ethyl acetate: CH_2Cl_2 3 to 1) to yield a yellow solid (0.282 g, 83% yield). ^{1}H-NMR (300 MHz, $CDCl_3$) d = 1.01 (t, 6H), 1.33 (mb, 14H), 1.68 (m, 4H), 1.93 (m, 2H), 2.39 (t, 4 H), 2.51 (m, 2H), 3.38 (t, 2H), 3.52 (s, trans-3H), 3.57 (s, cis-3H), 4.32 (m, cis-1H), 4.71 (m, trans-1H), 5.85 (m, cis-1H), 6.26 (m, trans-1H), 7.15 (s, 2H), 7.74 (t, 2H), 7.88 (s, 1H), 8.01 (t, 4H), 8.31 (sb, 4H), 8.83 (sb, 4H). ^{13}C NMR (300 MHz, $CDCl_3$) d = 14.4, 19.3, 24.5, 26.8, 27.4, 27.6, 27.9, 30.0, 31.1, 38.8, 56.2, 59.8, 71.5, 103.2, 107.1, 109.9, 111.4, 118.7, 136.6, 140.6, 146.2, 147.2, 150.7, 151.2, 159.0, 165.5, 172.6. MS (ESI): m/z (%) =673.6 (673.8 M+ calculated). Elemental Analysis calculated for $C_{37}H_{48}N_6O_6$: C 66.05, H 7.19, N 12.49, found: C 66.09, H 7.23, N 12.47

1-(12-methoxydodec-11-enyl)-1,3,5-triazinane-2,4,6-trione (32): 12-Bromo-1-methoxydodec-1-ene (0.453 g, 1.634 mmol) and cyanuric acid (1.054 g, 8.169 mmol) were combined in DMSO (50 mL) with K_2CO_3 (1.129 g, 8.169 mmol). The mixture was stirred under argon for 72 hours. The DMSO mixture was partitioned between ether (50 mL) and saturated $NaHSO_4$ (50 mL). The organic layer was collected, washed with brine, dried with $MgSO_4$ and reduced in volume to 30 mL. Addition of hexane formed a

white suspension which precipitated within 3 hours. The white solid was collect to yield the desired product (1.20 g, 45% yield). ^{1}H-NMR (300 MHz, $CDCl_3$) d = 1.33 (mb, 14H), 1.85 (m, 2H), 1.93 (m, 2H), 3.16 (t, 2H), 3.52 (s, trans-3H), 3.57 (s, cis-3H), 4.32 (m, cis-1H), 4.71 (m, trans-1H), 5.85 (m, cis-1H), 6.26 (m, trans-1H), 8.67(bs, 2H). ^{13}C NMR (300 MHz, $CDCl_3$) d = 24.5, 26.8, 27.4, 27.6, 27.9, 30.0, 31.1, 46.3, 56.2, 59.8, 103.2, 107.1, 146.2, 147.2, 152.7, 155.2. MS (ESI): m/z (%) = 326.2 (326.4 M+ calculated). Elemental Analysis calculated for C16H27N3O4: C 59.06, H 8.36, N 12.91, found: C 59.29, H 8.53, N 12.70.

(Z)-bis(3,5-bis(6-Propionamidopyridin-2-ylcarbamoyl)phenyl) tetracos-12-enedioate) (33): (Z)-Tetracos-12-enedioic acid (0.245 g, 0.665 mmol) and 5-hydroxy-*N1,N3*-bis(6-propionamidopyridin-2-yl)isophthalamide (0.836 g, 1.62 mmol) were combined in dry THF (60 mL). DCC (0.346 g, 1.662 mmol) and DMAP (0.020 g, 0.1662 mmol) were added to the solution. The mixture was refluxed overnight. The THF was removed and the resulting solid was purified by column chromatography (ethyl acetate: CH_2Cl_2 3 to 1) to yield a white solid (0.775 g, 87% yield). ^{1}H-NMR (300 MHz, CDCl3) d = 1.01 (t, 6H), 1.28 (mb, 24H), 1.68 (m, 4H), 1.79 (m, 4H), 2.39 (t, 4 H), 3.66 (t, 4H), 3.88 (t, 4H), 5.33 (dd, J = 4.9 Hz, 2H), 7.15 (s, 2H), 7.74 (t, 2H), 7.88 (s, 2H), 8.01 (t, 4H), 8.31 (sb, 4H), 8.83 (sb, 4H). ^{13}C NMR (300 MHz, CDCl3) d = 14.4, 19.3, 26.1, 27.5, 29.5, 29.6, 29.7, 29.9, 30.1, 32.9, 33.1, 38.8, 63.4, 71.5, 109.9, 111.4, 118.7, 130.1, 136.6, 140.6, 150.7, 151.2, 159.0, 165.5, 172.6. MS (ESI): m/z (%) = 1342.5 (1342.6 M+ calculated). Elemental Analysis calculated for $C_{74}H_{92}N_{12}O_{12}$: C 66.25, H 6.91, N 12.53, found C 66.31, H 6.92, N 12.49

General polymerization procedure for cyclooctene monomers: The desired CTA (usually 100 mg) was added to a dried three neck round bottom flask and $CHCl_3$ (5 mL) was added. The corresponding amount of **16** ([**16**]/[CTA] = 10, 20, 50, or 100) was added, followed by the addition **17** or **18** ([**16**]/[catalyst] = 4000) in $CHCl_3$. The solution was stirred for 72 hours at room temperature, and then precipitated in cold MeOH (10 mL) to yield the desired polymer. Polymers were collected by filtration and dried under vacuum before characterization.

General polymerization method for norbornene based monomers: 0.006 mmol of monomer is dissolved in 2 mL CH_2Cl_2, 0.6 μmol of **34** in solution is added to the reaction and stirred for 2 hours under argon. 12 μmol of CT is added and stirred for another 2 hours. The polymer is precipitated into cold MeOH and collected via filtration and dried under vacuum before characterization.

REFERENCES

[1] C. P. Wong, *Polymers for Electronic and Photonic Applications*, Academic Press Inc., **1993**.

[2] N. Hadjichristidis, M. Pitsikalis, S. Pispas and H. Iatrou, *Chem. Rev.* **2001**, *101*, 3747-3792.

[3] M. Kamigaito, T. Ando and M. Sawamoto, *Chem. Rev.* **2001**, *101*, 3689-3746.

[4] K. Matyjaszewski and J. Xia, *Chem. Rev.* **2001**, *101*, 2921-2990.

[5] J. H. K. Hirschberg, F. H. Beijer, H. A. van Aert, P. C. M. M. Magusin, R. P. Sijbesma and E. W. Meijer, *Macromolecules* **1999**, *32*, 2696-2705.

[6] J. H. K. Hirschberg, A. Ramzi, R. P. Sijbesma and E. W. Meijer, *Macromolecules* **2003**, *36*, 1429-1432.

[7] H. Hofmeier, A. El-ghayoury, A. P. H. J. Schenning and U. S. Schubert, *Chem. Commun.* **2004**, 318-319.

[8] K. Yamauchi, A. Kanomata, T. Inoue and T. E. Long, *Macromolecules* **2004**, *37*, 3519-3522.

[9] W. H. Binder, M. J. Kunz and E. Ingolic, *J. Polym. Sci., Part A: Polym. Chem.* **2004**, *42*, 162-172.

[10] W. W. Gerhardt, A. J. Zucchero, J. N. Wilson, C. R. South, U. H. F. Bunz and M. Weck, *Chemical Communications* **2006**, *20*, 2141-2143.

[11] W. H. Binder, M. J. Kunz, C. Kluger, G. Hayn and R. Saf, *Macromolecules* **2004**, *37*, 1749-1759.

[12] O. A. Scherman, G. B. W. L. Lighart, H. Ohkawa, R. P. Sijbesma and E. W. Meijer, *Proc. Natl. Acad. Sci. U. S. A.* **2006**, *103*, 11850-11855.

[13] J. Xu, E. A. Fogleman and S. L. Craig, *Macromolecules* **2004**, *37*, 1863-1870.

[14] E. A. Fogleman, W. C. Yount, J. Xu and S. L. Craig, *Angew. Chem. Int. Ed.* **2002**, *41*, 4026-4028.

[15] B. G. G. Lohmeijer and U. S. Schubert, *Angew. Chem. Int. Ed.* **2002**, *41*, 3825-3829.

[16] X. Wu and C. L. Fraser, *Macromolecules* **2000**, *33*, 4053-4060.

[17] R. H. Grubbs, *Handbook of Metathesis*, Wiley-VCH, **2003**.

[18] C. W. Bielawski, T. Morita and R. H. Grubbs, *Macromolecules* **2000**, *33*, 678-680.

[19] V. C. Gibson and T. Okada, *Macromolecules* **2000**, *33*, 655-656.

[20] T. Morita, B. R. Maughon, C. W. Bielawski and R. H. Grubbs, *Macromolecules* **2000**, *33*, 6621-6623.

[21] M. A. Hillmyer and R. H. Grubbs, *Macromolecules* **1993**, *26*, 872-874.

[22] H. S. Bazzi, J. Bouffard and H. F. Sleiman, *Macromoleclues* **2003**, *36*, 7899-7902.

[23] C. Burd and M. Weck, *Macromoleclues* **2005**, *38*, 7225-7230.

[24] R. J. Thibault, P. J. Hotchkiss, M. Gray and V. M. Rotello, *J. Am. Chem. Soc.* **2003**, *125*, 11249-11252.

[25] K. P. Nair, J. M. Pollino and W. M, *Macromoleclues* **2006**, *39*, 931-940.

[26] C. R. South, M. N. Higley, K. C.-F. Leung, D. Lanari, A. Nelson, R. H. Grubbs, J. F. Stoddart and M. Weck, *Chem. Eur. J.* **2006**, *12*.

[27] C. R. South, K. C.-F. Leung, D. Lanari, J. F. Stoddart and M. Weck, *Macromoleclues* **2006**, *39*, 3738-3744.

[28] J. M. Pollino, L. P. Stubbs and M. Weck, *J. Am. Chem. Soc.* **2004**, *126*, 563-567.

[29] M. Albrecht and G. Van Koten, *Angew. Chem. Int. Ed.* **2001**, *40*, 3750-3781.

[30] J. M. Pollino, L. P. Stubbs and M. Weck, *Macromolecules* **2003**, *36*, 2230-2234.

[31] J. Pollino and M. Weck, *Synthesis* **2002**, *9*, 1277-1285.

[32] W. T. S. Huck, L. Prins, J., R. H. Fokkens, N. M. M. Nibbering, F. C. J. M. van Veggel and D. N. Reinhoudt, *J. Am. Chem. Soc.* **1998**, *120*, 6240-6246.

[33] W. T. S. Huck, F. C. J. M. van Veggel, B. L. Kropman, D. H. A. Blank, E. G. Keim, M. M. A. Smithers and D. N. Reinhoudt, *J. Am. Chem. Soc.* **1995**, *117*, 8293-8294.

[34] B. M. J. M. Suijkerbuijk, M. Lutz, A. L. Spek, G. van Koten and R. J. M. Klein Gebbink, *Org. Lett.* **2004**, *6*, 3023-3026.

[35] J. M. Pollino and M. Weck, *Synthesis* **2002**, 1277-1285.

[36] J. M. Lehn, *Supramolecular Chemistry*, Wiley-VCH, **1995**.

[37] F. Ilhan, M. Gray and V. M. Rotello, *Macromolecules* **2001**, *34*, 2597-2601.

[38] J. Pranata, S. G. Wierschke and W. L. Jorgenson, *J. Am. Chem. Soc.* **1991**, *113*, 2810-2819.

[39] T. J. Murray and S. C. Zimmerman, *J. Am. Chem. Soc.* **1992**, *114*, 4010-4011.

[40] W. L. Jorgenson and J. Pranata, *J. Am. Chem. Soc.* **1990**, *112*, 2008-2010.

[41] Y. Kyogoku, R. C. Lord and A. Rich, *Proc. Natl. Acad. Sci. U. S. A.* **1967**, *57*, 250-257.

[42] L. P. Stubbs and M. Weck, *Chem. Eur. J.* **2003**, *9*, 992-999.

[43] R. J. Capon, C. Skene, E. H. Liu, E. Lacey, J. H. Gill, K. Heiland and T. Friedel, *J. Org. Chem.* **2001**, *66*, 7765-7769.

[44] S. Poulain, N. Noiret and H. Patin, *Tetrahedron Lett.* **1996**, *37*, 7703-7706.

[45] L. P. Stubbs and M. Weck, *Chem. Eur. J.* **2003**, *9*, 991-999.

[46] M. Pollino Joel and M. Weck, *Organic letters* **2002**, *4*, 753-756.

[47] M. A. Hillmyer, W. R. Laredo and R. H. Grubbs, *Macromolecules* **1995**, *28*, 6311-6316.

[48] L. P. Stubbs and M. Weck, *Chem. Eur. J.* **2003**, *9*, 992-999.

[49] Association constants were calculated by using the program Chem Equili, Version 6.1

[50] V. A. Bloomfield, D. M. Crothers and I. Tinoco, *Nucleic Acids: Structures, Properties and Functions;* University Science Books: Sausalito, **2000**.

[51] J. J. Storhoff and C. A. Mirkin, *Chem. Rev.* **1999**, *99*, 1849-1862.

[52] V. Berl, M. J. Krische, I. Huc, J.-M. Lehn and M. Schmutz, *Chem. Eur. J.* **2000**, *6*, 1938-1946.

[53] W. W. Zorbach and R. S. Tipson in *Procedures in Nucleic Acid Chemistry*, *Vol. 1* Interscience, New York, **1968**, pp. 83-84.